

Supplementary Materials

Effects of Central Metal Ion on Binuclear Metal Phthalocyanine-Based Redox Mediator for Lithium Carbonate Decomposition

Qinghui Yan ^{1,4,†}, Linghui Yan ^{3,†}, Haoshen Huang ², Zhengfei Chen ², Zixuan Liu ^{2,4,*}, Shaodong Zhou ^{3,*} and Haiyong He ⁴

¹ School of Materials Science and Chemical Engineering, Ningbo University, Ningbo 315211, China; 2111086218@nbu.edu.cn

² School of Biological and Chemical Engineering, NingboTech University, Ningbo 315100, China; 13685729957@163.com (H.H.); zhengfei.chen@nbt.edu.cn (Z.C.)

³ College of Chemical and Biological Engineering, Zhejiang University, Hangzhou 310058, China; lhyan@zju.edu.cn

⁴ Ningbo Institute of Materials Technology and Engineering, Chinese Academy of Sciences, Ningbo 315201, China; hehaiyong@nimte.ac.cn

* Correspondence: liuzixuan@nbt.edu.cn (Z.L.); szhou@zju.edu.cn (S.Z.);
Tel.: +86-574-882-295-98 (Z.L.); +86-571-879-516-15 (S.Z.)

† These authors contributed equally to this work.

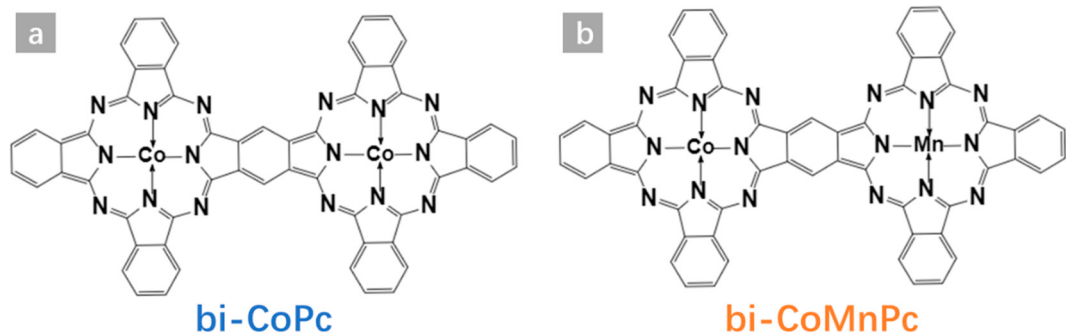


Figure S1. The structures of bi-CoPc and bi-CoMnPc

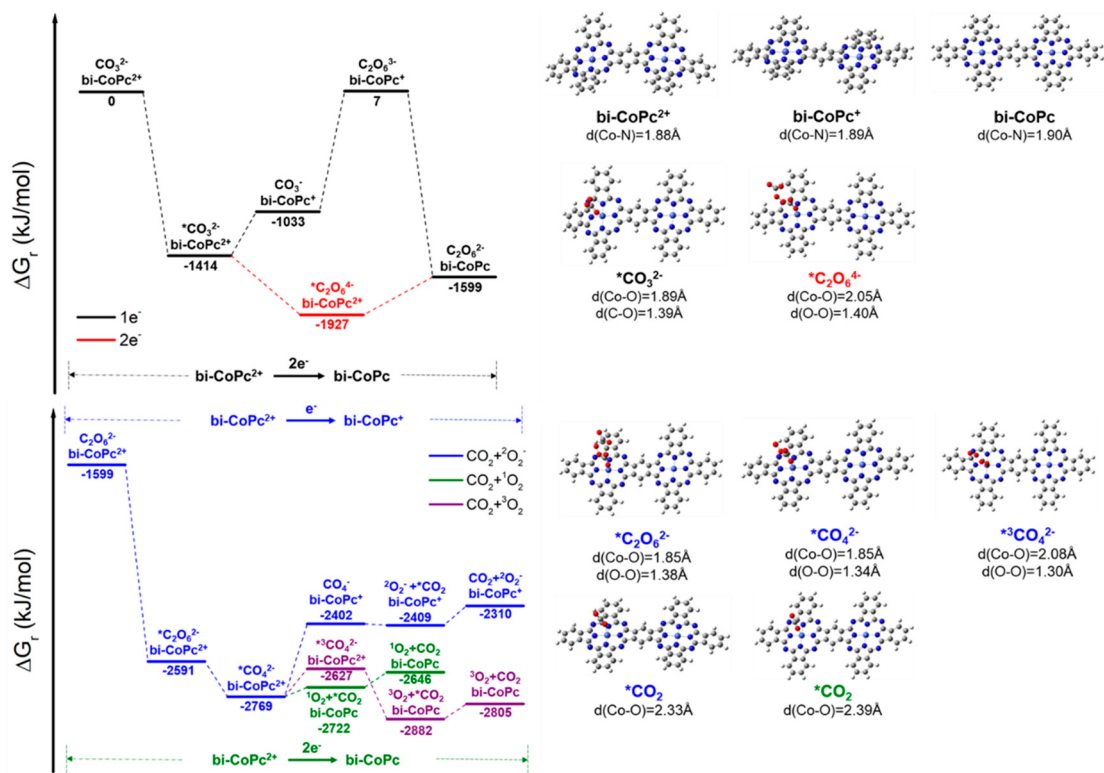


Figure S2. The Li_2CO_3 decomposition pathways on bi-CoPc^{2+} and corresponding structures with $\text{bi-CoPc}^{2+} \rightarrow \text{bi-CoPc}$

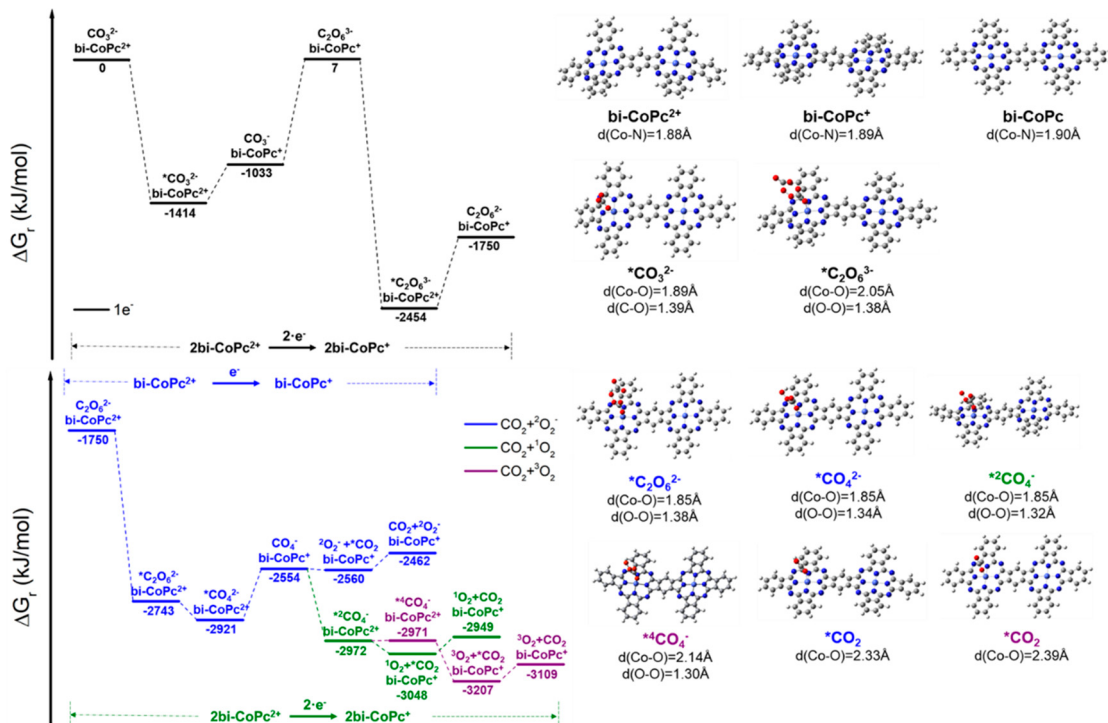


Figure S3. The Li_2CO_3 decomposition pathways on pristine bi-CoPc^{2+} and the corresponding structures with $2\text{bi-CoPc}^{2+} \rightarrow 2\text{bi-CoPc}^+$

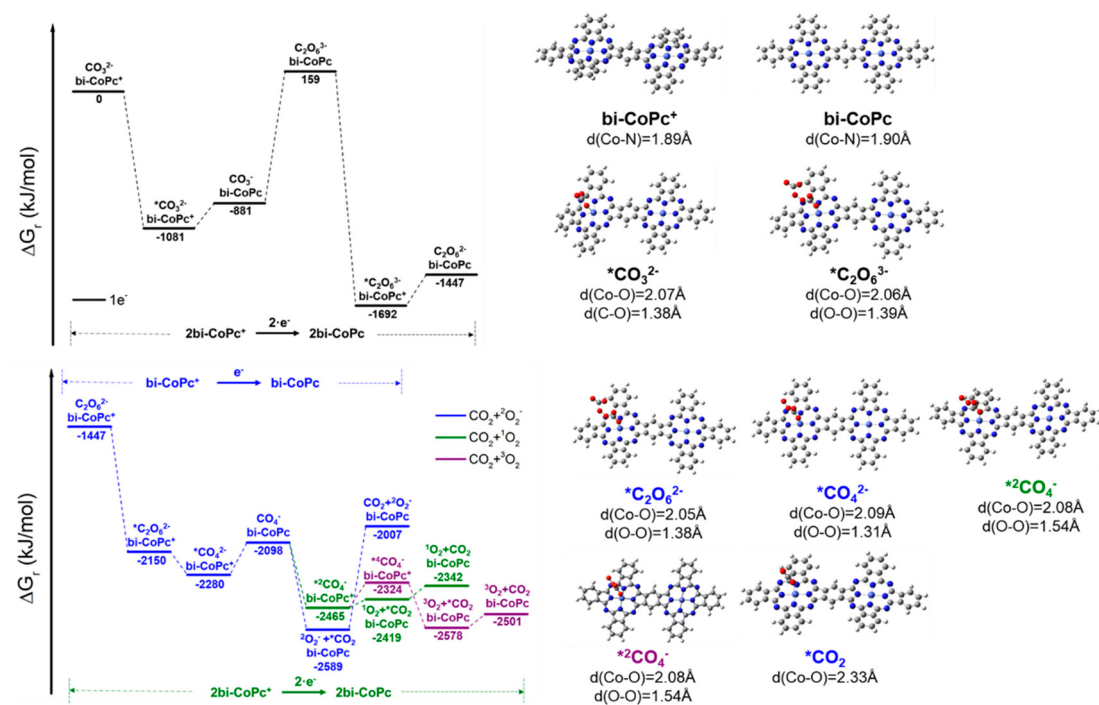


Figure S4. The Li_2CO_3 decomposition pathways on bi-CoPc^+ and the corresponding structures with $2\text{bi-CoPc}^+ \rightarrow 2\text{bi-CoPc}$

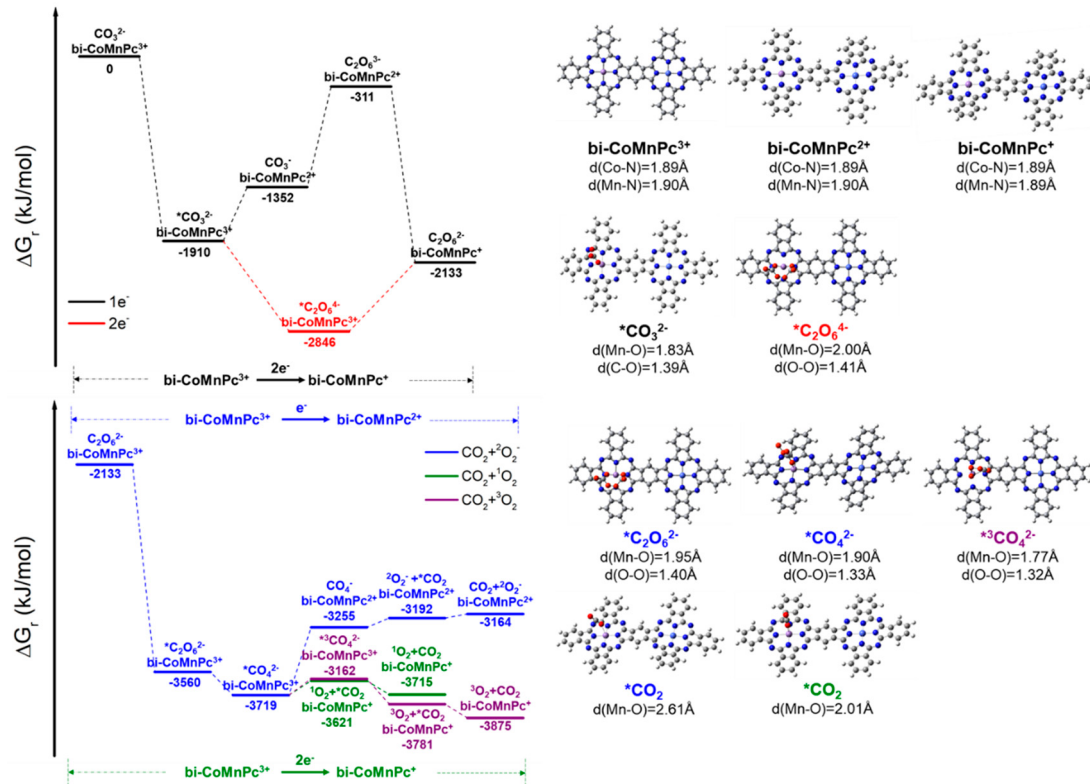


Figure S5. The Li_2CO_3 decomposition pathways on pristine bi-CoMnPc^{3+} and the corresponding structures with $\text{bi-CoMnPc}^{3+} \rightarrow \text{bi-CoMnPc}^+$

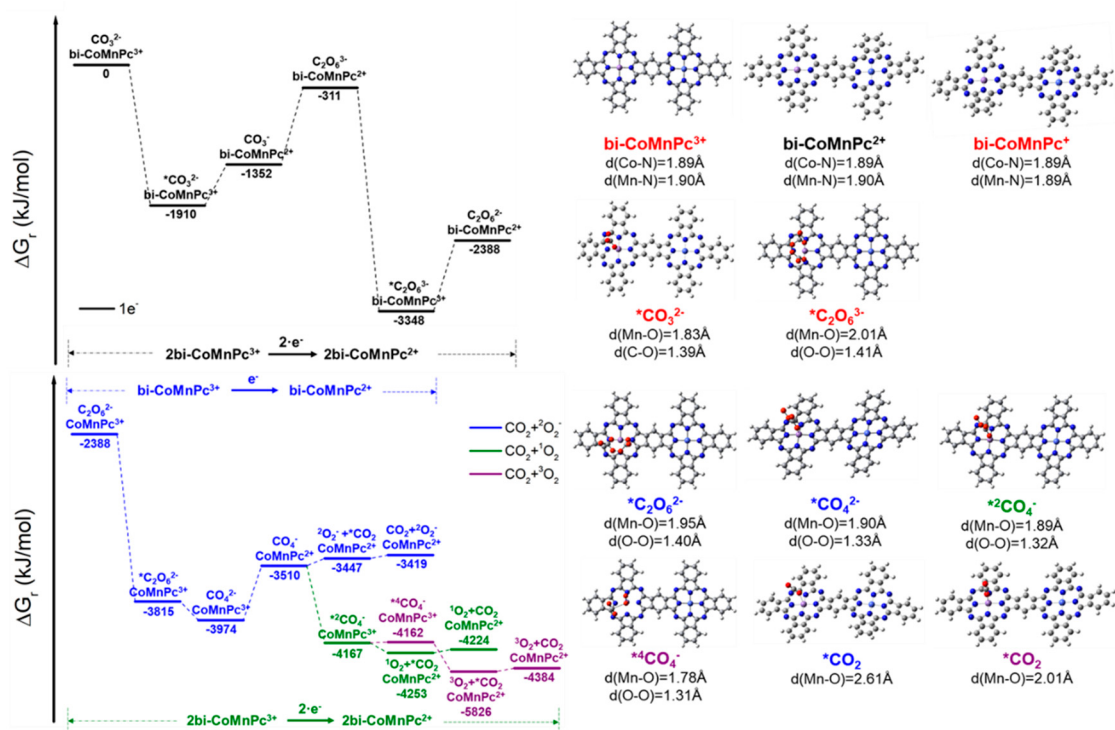


Figure S6. The Li_2CO_3 decomposition pathways on pristine bi-CoMnPc^{3+} and the corresponding structures with $2\text{bi-CoMnPc}^{3+} \rightarrow 2\text{bi-CoMnPc}^{2+}$

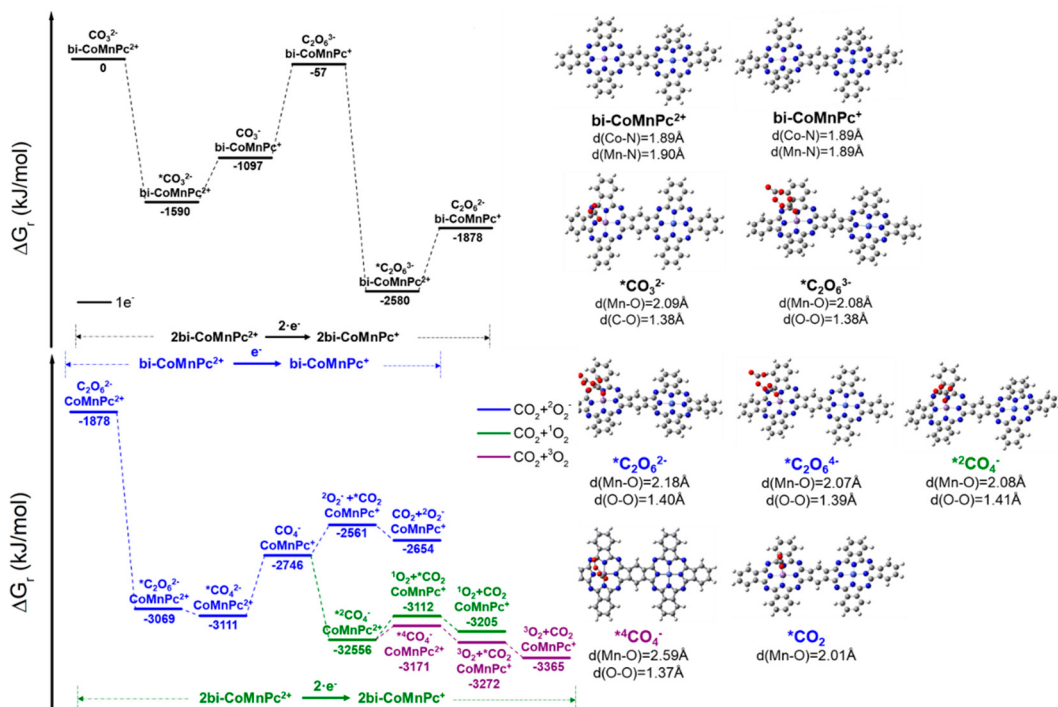


Figure S7. The Li_2CO_3 decomposition pathways on pristine bi-CoMnPc^{2+} and the corresponding structures with $2\text{bi-CoMnPc}^{2+} \rightarrow 2\text{bi-CoMnPc}^{+}$

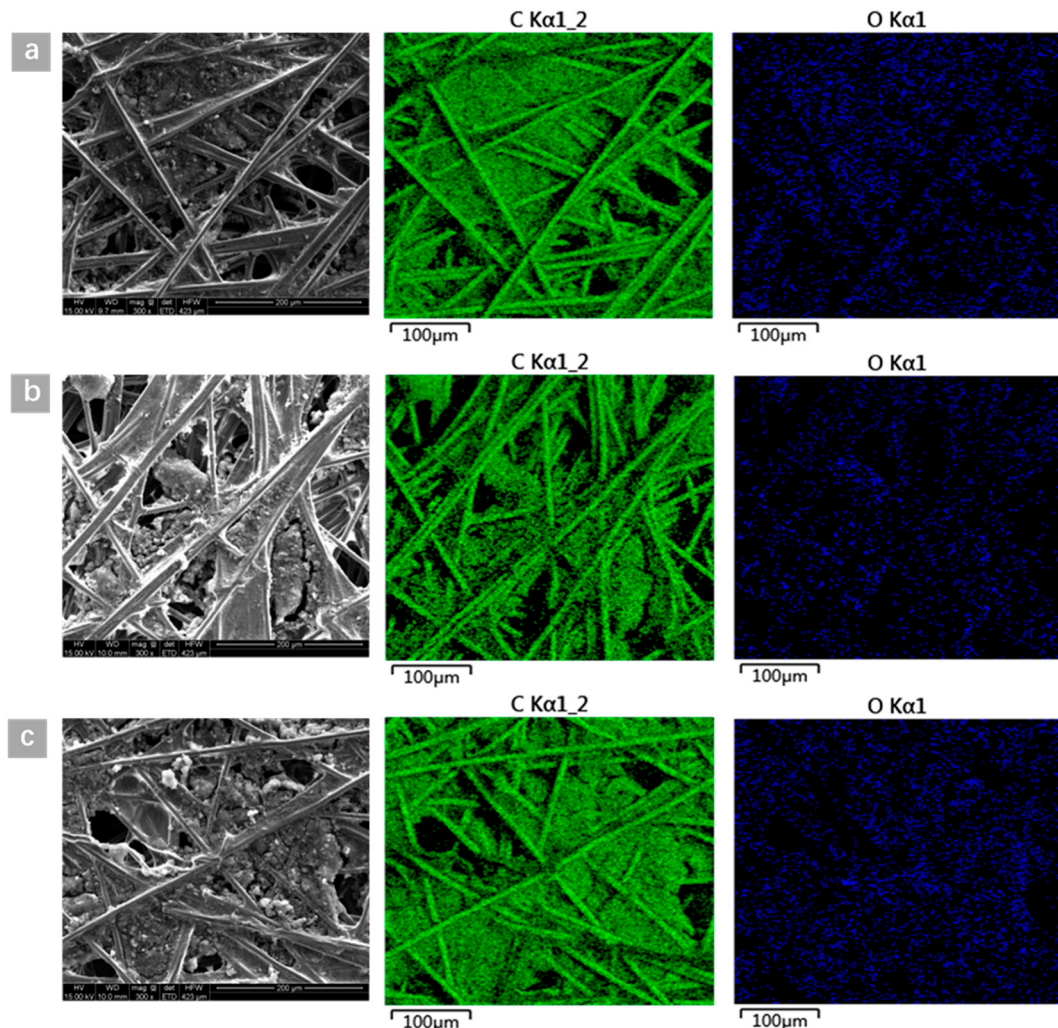


Figure S8. The SEM images and EDS mapping results of carbon and oxygen for the air cathode (a) without RM, (b) with bi-CoPc and (c) with bi-CoMnPc after 1 discharge-charge cycle.

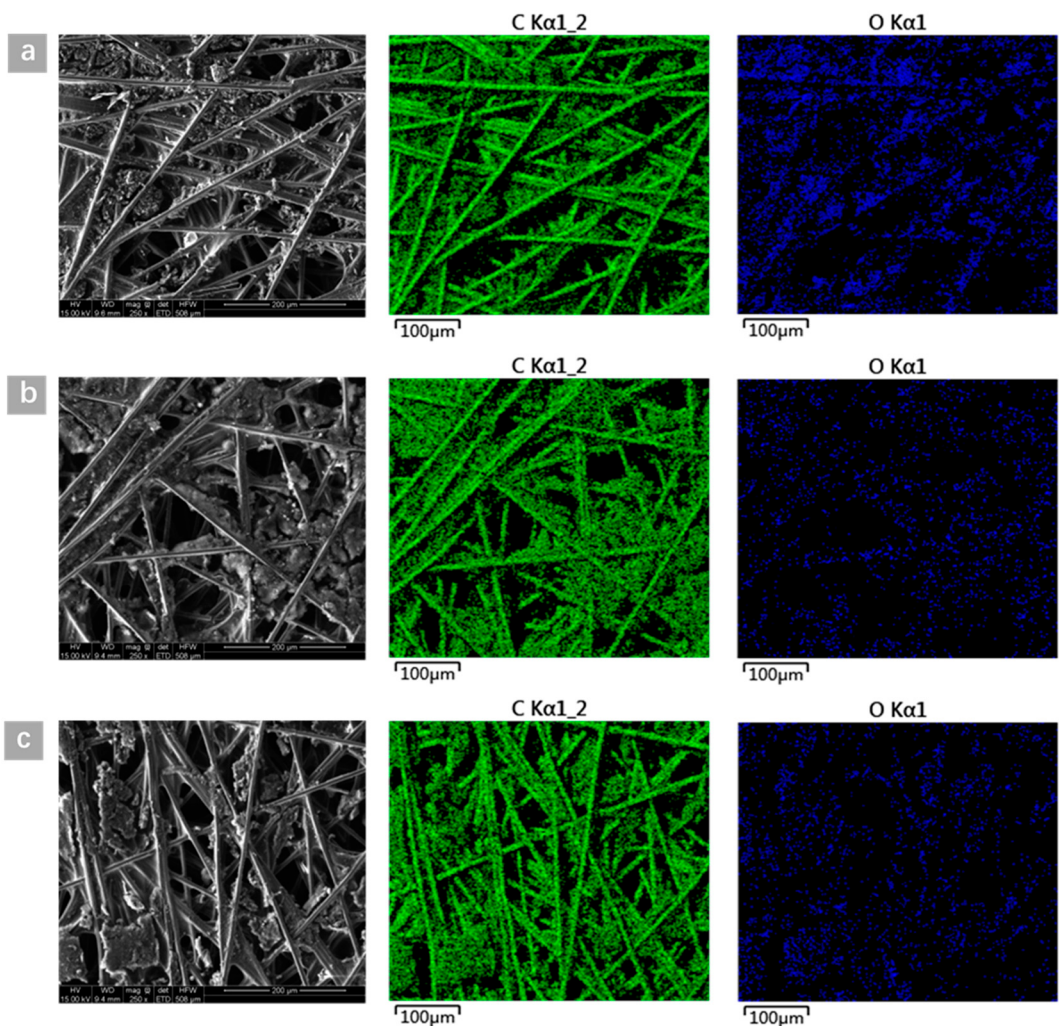


Figure S9. The SEM images and EDS mapping results of carbon and oxygen for the air cathode (a) without RM, (b) with bi-CoPc and (c) with bi-CoMnPc after 10 discharge-charge cycles.

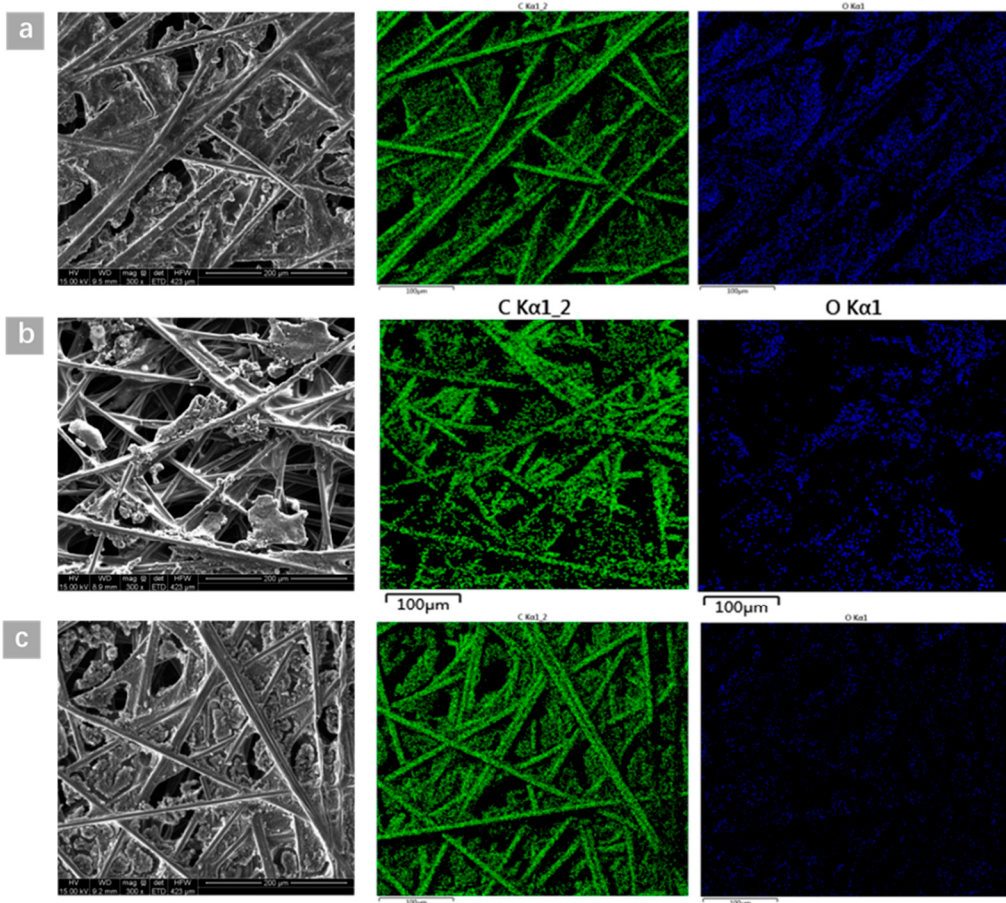


Figure S10. The SEM images and EDS mapping results of carbon and oxygen for the air cathode (a) without RM, (b) with bi-CoPc and (c) with bi-CoMnPc after 30 discharge-charge cycles.

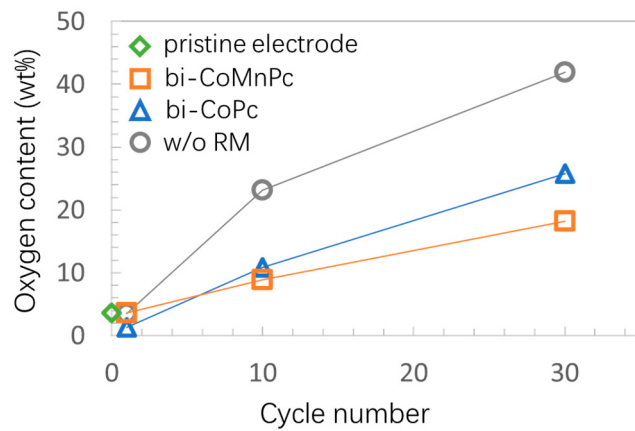


Figure S11. The oxygen content in the cycled air cathodes according to EDS results.